

KEK Preprint 98-170
October 1998
R

Description of
Multilayered Gamma-Ray Exposure Buildup Factors
up to 40 mfp by the Approximating Model

Kazuo SHIN and Hideo HIRAYAMA



** To be published in J. Nucl. Sci. Technol.*

High Energy Accelerator Research Organization (KEK), 1998

KEK Reports are available from:

Information Resources Division
High Energy Accelerator Research Organization (KEK)
1-1 Oho, Tsukuba-shi
Ibaraki-ken, 305-0801
JAPAN

Phone: 0298-64-5137
Fax: 0298-64-4604
Cable: KEK OHO
E-mail: Library@kekvox.kek.jp
Internet: <http://www.kek.jp>

Description of Multilayered Gamma-Ray Exposure Buildup Factors up to 40 mfp by the Approximating Model

Kazuo SHIN

*Department of Nuclear Engineering, Kyoto University
Yoshida, Sakyou-ku, Kyoto 606-8317, Japan*

And

Hideo HIRAYAMA

*High Energy Accelerator Research Organization
1-1 Oho, Tsukuba-shi, Ibaraki 305-0801 Japan*

Abstract

An approximating formula recently proposed by the authors for gamma-ray buildup factors of multilayered shields was applied for very thick shields up to 40 mfp. For this purpose, modifications were made to the model and the fitting method to improve the data reproducibility. The previous model was expanded so that it included both the plane normal and point isotropic geometries.

The verification test of the modified model was made for three materials; water, iron and lead. The separately published data of double-layered shields for point isotropic buildup factors calculated by EGS4 from 0.1 MeV to 10 MeV were used as well as newly calculated data at 1 MeV for the plane-normal geometry, and data for the point isotropic geometry of triple-layered shields at 1 and 10 MeV.

The present formula generally shows a very good reproducibility of the multilayer buildup factors, even in case of very thick shielding problems. The observed error between the approximating description and the EGS4 data is 15% in the intermediate energy range, about 30% in the higher energy range, and 35% at 0.3 MeV. However, the error in the approximation reaches a factor of 4 in the worst case at 0.1 MeV.

I INTRODUCTION

The point kernel method has been widely used in gamma-ray shielding design. The shields and equipments used in nuclear facilities are composed of various component materials. Therefore, it has been desired to enable the use of multilayer buildup factors in point kernel codes. Correspondingly, many studies^{(1)–(9)} have been conducted to express the multilayered buildup factors by simple expressions so that they may be parameterized by these formulae and incorporated in the point-kernel codes.

These formulae proposed so far^{(1)–(9)} have tried to describe multilayer buildup factors as combinations of those of the composing materials. Unfortunately, the buildup factor in multilayered materials shows a very complex behavior, reflecting changes in the gamma-ray energy spectrum in the shield from one material to the other. Since the buildup factor of the monolayered shield contains only integrated information about the spectrum in the

material, the combinations of the buildup factors of monolayered materials can reflect a spectrum change in the multilayered material only in an indirect manner. As a result, these formulae succeeded in reproducing the multilayer buildup factor only for specific cases.

In our previous papers^{(10),(11)} we proposed a new model having the vector form which explicitly included energy spectrum information in the model. The model was successfully applied to double- and triple-layered shield problems up to 10-mfp(mean free path) thickness at energies from 0.5 to 10 MeV.

The objectives of the present study are to make some modifications to the model so that the model may better reproduce reference buildup factors even for very thick shielding problems up to 40 mfp, then to test the modified model by using the results of the electron and gamma-ray shower code EGS4⁽¹²⁾ calculations obtained by the new technique.^{(13),(14)}

In our previous papers, the approximating model was developed to describe buildup factors of the plane normal geometry⁽¹⁰⁾ first, and the model was changed to be applied to the point isotropic geometry⁽¹¹⁾. In the present work, these are unified to a single model that includes the both geometries.

Our approximating description of buildup factors for the point isotropic geometry contains the radius dependence of the probabilities of the transmission through and backscattering from a one-mfp-thick material shell, which has been expressed by simple analytical expressions that include empirical parameters. The parameters for the albedo were assumed to be common for all of the materials⁽¹¹⁾ to minimize the number of parameters. However, errors caused by this assumption was no longer trivial in the case of the very thick shield problems. Therefore, those parameters of the albedos were treated as being material dependent in this work in order to improve the data reproducibility.

The empirical parameters included in the model were determined in previous papers^{(10),(11)} by fitting the expression to buildup factors of double-layered shields. Therefore, the parameters of the three materials were determined in two steps, using the data of the double-layered shields composed of materials 1 and 2, and then those of materials 1 and 3. When the sequence of the fitting was changed, the fitted parameters slightly varied, which somewhat affected the composed buildup factors.

Here, in the present study, the parameters of three materials were determined simultaneously by fitting the expression to all of the buildup factors of possible combinations for double-layered shields of the three materials, i.e. materials 1 and 2, materials 1 and 3, and materials 2 and 3. This process decreases the ambiguity in determining the parameters, caused by the selection of the combination of two materials and sequence of the fitting.

Finally, the modified model was tested by buildup factors of double-layered shields listed as tables in Ref.14, where three materials(water, iron and lead) were assumed in the calculations. The data at 0.1, 0.3, 0.6, 1, 3, 6 and 10 MeV of the point isotropic geometry were utilized. In addition to the above data, buildup factors up to 35-mfp depth at 1 MeV of the plane geometry, and those of the point isotropic geometry for 40-mfp-thick triple-layered shields at 1 and 10 MeV were generated in this work.

The present paper is organized as follows. Section 2 gives an outline of the present model. Section 3 gives the results of a feasibility test of the model based on the data for 40-mfp-thick shields. The final section contains conclusions.

II DESCRIPTION OF APPROXIMATION MODEL OF BUILDUP FACTORS

II.1 Outline of the Approximating Model

We use the vector form to express the energy spectrum of gamma-rays, dividing the energy range from 0 to the source energy (E_0) into 4 discrete groups.

A multilayered shield of thickness r of N materials, i.e. n_1 -mfp-thick material 1, n_2 -mfp-thick material 2, and so on, is considered. This shield is followed by an infinite medium of material N. In the point isotropic geometry, the shield is a sphere of radius r , and a point isotropic gamma-ray source is located at the center of the shield. For the plane geometry, the shield is a plane of thickness r , and a broad beam of gamma-rays is injected normal to the plane.

The dose buildup factor (B_D) at depth r is given by

$$B_D = \vec{C}(I + B_N)\left(\prod_{l=1}^N T_l^{n_l}\right)\vec{S} \quad , \quad (1)$$

where \vec{S} is a source intensity vector, whose explicit expression is $\vec{S} = (1, 0, 0, 0)$, T_l the transmission matrix of material l , n_l is the thickness of the material l in mfp unit, B_N the albedo matrix for the outside material (N), I the unit matrix, and \vec{C} the conversion vector from the energy-fluence index to the dose index.^{(10),(11)}

The transmission matrix (T) is defined with a 1-mfp-thick shell for each material, which depends on the radius of the shell in the point-isotropic case. The matrix is calculated by

$$T_{ij} = fK \frac{\phi_{ij}}{\phi_{11}} \quad , \quad (2)$$

where T_{ij} is the ij -element of matrix T, and ϕ_{ij} is the group-averaged transmitted flux in the i 'th group for the incidence of the j 'th group source of the unit intensity. For the detailed definition and assumptions for the calculation of ϕ_{ij} , see Refs. 10 and 11.

The factor K in Eq.(2) is a correction factor for not considering the angular distribution of gamma-rays in the model, and is given as K is $1(j = 1)$, $\alpha(j = 2)$, $\beta(j = 3)$ and $\gamma(j = 4)$, where α, β, γ are empirical parameters determined by the least-squares method, so that the expression (1) gives the best fit to the data of the buildup factors.

The factor f in Eq.(2) is set to be unity for the plane normal geometry, and to be f_p for the point isotropic geometry, where f_p describes the shell-curvature dependence of the gamma-ray transmission probability in spherical geometry, and is defined as $f_p = 1(i = 1)$, $R_1(i = 2, 3)$, and $R_2(i = 4)$. The factors $R_l(l = 1, 2)$ are a function of radius that contains two fitting parameters (a_l and b_l).⁽¹¹⁾

We approximated^{(10),(11)} the infinite albedo matrix ($B_N(r)$) of Eq.(1) by a finite medium one; a 1-mfp-thick shell of material N which was a spherical shell of a 1-mfp-inner radius in the case of the point isotropic geometry. The ij -element ($(B_N)_{ij}$) of the albedo matrix is given by

$$(B_N)_{ij} = g \frac{\int_{E_i} \phi_B(E) \eta(E) dE}{\eta_i} \quad , \quad (3)$$

where $\phi_B(E)$ is the reflected gamma-ray flux from the shell, while assuming normal incidence of the j 'th-group gamma-rays of the unity intensity, $\eta(E)$ is the fluence-to-dose conversion factor at the energy E , and η_i an i 'th group averaged one of $\eta(E)$.

The factor g in Eq.(3) is a geometrical factor so as to modify the calculated albedo matrix to be used for a given depth; g is unity (plane normal geometry), and g_p (point isotropic geometry), where g_p describes the dependence of the albedo on the radius (r) at the given depth in spherical geometry. This is explicitly given by

$$g_p = \left\{ 1 - \frac{b_B}{\left(\frac{r}{r_0} + h\right)^{a_B}} \right\} / \left\{ 1 - \frac{b_B}{(1+h)^{a_B}} \right\}, \quad (4)$$

where r_0 is the 1-mfp-thickness of material N. The parameter h was empirically set as 0.5 in the previous model⁽¹¹⁾. However, since the albedo should approach to zero when the radius (r) approaches zero, we changed the expression of h in this work so that $g_p = 0$ at $r = 0$;

$$h = b_B \left(\frac{1}{a_B} \right). \quad (5)$$

The empirical parameters (a_B and b_B) are considered as material dependent in this paper and are estimated from the least squares-fitting procedure described below.

II.2 Calculation of the Matrices and Determination of the Empirical Parameters

The group structure used in this work is one tested in Ref. 11. This group structure puts more emphasis on the higher energy range, and the width of the group becomes rather wider in the lower energy range.

With this group structure, we calculated the transmission matrix using the EGS4 code⁽¹²⁾. A 1-mfp-thick slab was used to calculate the matrix of the slab geometry, assuming a source of unit intensity normally incident to the slab. On the other hand, to calculate the matrix of the point isotropic geometry, a 1-mfp-radius sphere was used, assuming a source of unity intensity at its center. The albedo matrix was also calculated using EGS4 and the same conditions as described above in the slab geometry. In the point isotropic geometry, an albedo calculation was made for a 1-mfp-thick shell with an inner radius of the 1-mfp length, where gamma-rays were injected normal to the inner surface. The obtained albedo values were renormalized so that the buildup factor at the 1-mfp depth would exactly reproduced by formula (1).

Expression (1) contains the empirical parameters α , β and γ included in K , a_l , b_l ($l = 1, 2$) in R_l , and a_B , b_B of Eq.(5). These parameters are assumed to be both material and energy dependent. It is noted that three materials (water, iron and lead) were assumed in this work. All of the parameters were determined by the least-squares method at each energy so as to simultaneously fit expression (1) to the reference buildup factors of all single- and double-layered shields comprising the considered materials.

To determine the parameters of materials 1, 2 and 3, we considered three combinations of these materials: materials 1 and 2, materials 2 and 3, and materials 1 and 3. Also, for each of the material combinations, we use reference data of the four material configurations of N -mfp thickness. For example, the configurations considered for the combination of materials 1 and 2 were single-layered shields of both materials, a double-layered shield of the n -mfp material 1 followed by material 2, and the same thickness shield with the reversed order of the material arrangement. We prepared three sets of the above-mentioned data, where the thickness of the 1st layer was changed threefolds: $n(1)$, $n(2)$ and $n(3)$ mfp.

We defined the square of the relative difference in buildup factors W by

$$W = \sum_{l=1}^3 \sum_{m=1}^4 \sum_{k=1}^3 \sum_{n'=n(k)}^N \left[\left\{ \frac{B_m(n') - B_{0m}(n')}{B_{0m}(n')} \right\}^2 + \left\{ \frac{B_m(n') - B_{0m}(n')}{B_m(n')} \right\}^2 \right], \quad (6)$$

where $B_m(n')$ = the buildup factor given by Eq.(1) at a depth of n' mfp; $B_{0m}(n')$ = the corresponding reference data; $n' = n(k)$ to N , representing depths after the material boundary, where $n(k) = 1$ for the monolayered materials; $k = 1$ to 3, representing the three different first-layer thicknesses; $m = 1$ to 4, representing the above four material configurations; $l = 1$ to 3, representing the three combinations of materials. The summation on l means the fitting of the buildup factors for all kinds of double-layered shields that can be made up by three materials.

The value of W is a function of 27 parameters ($\alpha, \beta, \gamma, a_1, b_1, a_2, b_2, a_B$ and b_B) of materials 1, 2 and 3. These 27 parameters were simultaneously changed gradually in a direction where the value W most quickly approached the minimum one until W became less than a predetermined small value.

In all cases of point isotropic sources, we used $N = 40$ and $n(1) = 5, n(2) = 10$ and $n(3) = 20$ as described in Ref. 14, whereas $N = 35$ and $n(1) = 5, n(2) = 10$ and $n(3) = 21$ were used for the plane source.

III APPLICATION OF THE EXPRESSION TO THE MULTILAYER BUILDUP FACTORS

III.1 Application of the Expression to the Multilayered Slab Geometry

The buildup factors of 1-MeV gamma-rays normally incident to a slab in the plane geometry were calculated using EGS4 for single- and double-layered shields of material combinations of water, iron and lead, whose total thickness was 35 mfp and 1st-layer thickness was 5, 10 and 21 mfp. The present approximating model was applied to the obtained buildup factor data. Since the plane geometry was used, the fitting parameters were only α, β and γ in the factor K .

The results of the data fitting are given in Figs.1 through 3 for shields composed of water and lead, water and iron, and iron and lead, respectively.

Figure 1 shows a comparison of the reproduced buildup factors by the present model along with reference data for the double-layered shields comprising water and lead shields. The data reproduced by the present model agree quite well with those by the EGS4 calculation. In more detail, a discrepancy of 16% at maximum is seen in the data of the shields of 21-mfp water followed by lead. However, the difference in this amount is acceptable for an approximating expression of the buildup factor, which may be used in routine shielding designs.

Because the albedo of gamma-rays differs largely between water and lead, the buildup factor of double-layered shields at the material boundaries differs from the corresponding values of the monolayered shields. This behavior of the buildup factor of the double-layered shields is very well reproduced by the present model.

A comparison of the data reproduced by the present model with the reference ones for shields comprising water and iron is shown in Fig.2. The overall agreement between them is very good. The largest disagreement of 12% between them is seen in the data of the double-layered shield of 21-mfp water followed by iron. Low-energy gamma-rays which are built up in the water shield are quickly absorbed in the first few-mfp of a thick shield of

iron, which is moderately reproduced by the present model. The 12% discrepancy shown in Fig.2 is not a serious problem for the approximating model. However, if we desire to express the behavior of the buildup factor exactly in this transient region, the number of groups must be increased. The same thing may be pointed out for the similar discrepancy already seen in Fig. 1 concerning the data of a shield of 21-mfp thick water followed by lead.

Results for shields comprising iron and lead are given in Fig.3, where data based on the present model are compared with the reference data obtained by EGS4. Again, the agreement between them is satisfactory. The maximum amount of disagreement between them is 10%, which is seen at a 35-mfp thickness for a shield of 21-mfp thick iron followed by lead.

III.2 Application of the Model to Point Isotropic Buildup Factors

The behavior of the buildup factor strongly depends on the gamma-ray energy, reflecting the change in the linear attenuation coefficient and production rates of secondary photons, such as bremsstrahlung and fluorescence. Correspondingly, the gamma-ray energy where the buildup factor shows typical behaviors can be classified into three regions: low-, intermediate- and high-energy ranges. Therefore, results of an application test of the present model is discussed for each of these energy ranges.

III.2.1 Intermediate Energy Range

The energy range from 0.5 MeV up to 3.5 MeV is the most important one for applying the point kernel method, where major gamma-ray sources are included. The Compton scattering dominates the gamma-ray reaction in this energy range, and the linear attenuation coefficient decreases with rising the gamma-ray energy. Below 1 MeV, the photoelectric cross section increases quickly with lowering the energy. Generally, the the buildup factor in this energy range becomes larger with decreasing the atomic number.

Typical results of the present model in this energy range are shown in Fig. 4 for double-layered shields comprising water and iron at 1 MeV. When the figure is compared with the corresponding one of Fig. 2 for the plane geometry, a very different behavior of the point isotropic buildup factor is clearly seen.

The length corresponding to 1 mfp at 1 MeV is very different between water and iron, whereas the difference in the buildup factor is not very large between the two materials. Under this condition, the buildup factors of the double-layered shields of iron followed by water show an excess over the corresponding buildup factor of the water shield, and those of the shields of water followed by iron fall below the iron data. These behaviors of the reference buildup factors as well as the absolute values are quite well reproduced by the current model.

An example of data fitting by the present model at 3 MeV is shown in Fig. 5 for double-layered shields of water and lead. At this energy, the difference in the value of the buildup factor is not large, even between water and lead. A buildup factor of 20-mfp lead followed by water shows an interesting behavior. When the material is switched from lead to water, it increases quickly and goes over the corresponding values of water, then approaches to the buildup factor of water again. All data in the figure are reproduced by the present model quite well, except for the very small discrepancies seen just after the boundaries from water to lead.

In general, the reproducibility of the buildup factor in this energy range by the present model is very good. The maximum observed error of the approximation is about 15% for all of the tested cases of double-layered shields at 0.6, 1 and 3 MeV. The error is largest at 0.6 MeV, and smallest at 1 MeV.

The buildup factors of triple-layered shields were calculated using the EGS4 code at 1 MeV. The applied shields are of 40-mfp thickness and having the following configuration: 8-mfp water + 4-mfp iron + lead, 8-mfp iron + 4-mfp lead + water, and 8-mfp lead + 4-mfp water + iron. The buildup factors of these shields were reproduced by the present model by using pre-determined parameters obtained by using the data of double-layered shields. The thus-composed results are compared with the corresponding data of the EGS4 calculations in Fig. 6. It can be seen in the figure that the data of all material configurations are very well reproduced by the present model, except for a small discrepancy seen near to the material boundaries from lighter materials to lead.

III.2.2 High-Energy Range

In the high-energy range, i.e. $E_\gamma \geq 6$ MeV, the linear attenuation coefficient of heavy materials, like lead, increases with the gamma-ray energy due to an increase in the pair-production cross section. Therefore, scattered photons down to the Compton minimum energy have a greater probability of penetration through the shield than do photons at the source energy. Moreover, the bremsstrahlung production cross section is fairly large for high-energy electrons in lead. This increases the number of photons near and below the Compton minimum energy. It is noted that the critical energy in lead is 7 MeV, which means that the multiplication of photons may take place by a cascade reaction at 10 MeV in the lead shield. Consequently, the buildup factor in lead becomes very large at deep locations. In general, the buildup factor in this energy range becomes larger in the order of the atomic number of the material, which means that the buildup factor of water is the smallest of water, iron and lead.

The results of the present model at 10 MeV are compared with the reference data of EGS4 in Fig. 7, where the buildup factors of shields comprising water and lead are shown. The buildup factors in the lead shields, both in the single- and double-layered shields, increase very quickly with increasing the lead thickness. This behavior of the buildup factor in the lead shield is very well reproduced by the present model in Fig. 7.

However, the buildup factor in the water shield is slightly underestimated by the present model, especially in double-layered shields. The maximum amount of the discrepancy observed between the two data is $\sim 30\%$, which is observed at 6~20 mfp thicknesses in water shields. The gamma-ray spectrum in lead is very soft, compared with the hard spectrum in water. This spectrum change from lead to water may not be very well reproduced by the present model, because of the 4-group approximation.

The point isotropic buildup factors at 10 MeV of triple-layered shields were calculated using EGS4. The shields considered were 8-mfp water + 4-mfp iron + lead, 8-mfp iron + 4-mfp lead + water, and 8-mfp lead + 4-mfp water + iron. The parameters already determined using the data for the double-layered shields were used in the present model to compose the buildup factors of the triple-layered shields.

The thus-obtained results are compared with the corresponding ones from EGS4 in Fig. 8. The buildup factors of the triple-layered shields based on the present model agree quite well with those from the EGS4 calculation except for at around 20 mfp in water of a shield of iron + lead + water, where the present model underestimates the buildup factor by about

30%. This underestimation corresponds to the underestimation seen for the double-layer data in the water region of Fig. 7.

The behaviors of the buildup factors at 6 MeV were quite similar to those at 10 MeV. However, the reproducibility of the data by the present model was improved. The underestimation observed in the water shields was resolved at 6 MeV.

III.2.3 Low-Energy Range

In the low-energy range, i.e. 0.1 and 0.3 MeV, the absorption cross section is generally very large, except for light materials. This causes a hardening of the gamma-ray spectrum in the shields, and almost no gamma-rays exist in the 4th group. Corresponding to this, the correction factor (f_p) defined in section II.1 is changed in this energy range: $f_p = 1$ ($i = 1$), R_1 ($i = 2$), R_2 ($i = 3$), and 1 ($i = 4$).

On the other hand, in the water shield, low-energy gamma-rays buildup in the 4th group very quickly, which results in large values of the buildup factor at deep locations. Nevertheless, the above definition of f_p is also used for water. Generally, the characteristics of the buildup factor differ very much in this energy range, depending on the material. It should be noted that when the original definition of f_p was used instead of the above one, the obtained results were similar to, but slightly worse than those given by the above one. All of the data described below were fitted results with f_p as defined above.

An example of the results of the present model at 0.3 MeV is shown in Fig. 9 for shields comprising water and lead. The water buildup factor becomes as large as 5×10^3 at 40-mfp depth, whereas that of lead stays at about 2, even at the deepest location. The reproducibility of the data based on the present model is satisfactory.

In the case of double-layered shields of iron and lead, an $\sim 35\%$ disagreement, which was the largest error observed of all cases at 0.6 MeV, was seen between the present model and the reference data in the lead shields behind iron.

It was already reported⁽²⁾ that the buildup factor of lead at 0.1 MeV increased very quickly with increasing the lead thickness, and reached a value of as large as $\sim 10^{11}$ at 40-mfp thickness. On the other hand, the buildup factor of iron at the same energy remained at a very small value, even for a very thick shield. The water buildup factor at this energy becomes as large as 3×10^4 at 40-mfp thickness, and much larger than at higher energies.

These extreme behaviors of the buildup factor were caused by changes in the gamma-ray spectrum in the shields. The intense absorption characteristics remove low-energy gamma-rays in iron, and form the very hard spectrum, whereas in water, the low-energy gamma-rays buildup greatly, due to the low absorption cross section. The existence of the K- and L-edges, and the production of fluorescences changes the situation very differently in lead, where the produced secondary photons penetrate the lead shield via the cross section windows just below the edges.

As explained, the spectrum difference of gamma-rays in these materials is very large at 0.1 MeV, and the few group spectrum expression of the present model may no longer be valid. Therefore, it is interesting to test whether or not the present model works at 0.1 MeV.

The buildup factor for the combination of iron and lead is shown in Fig. 10, which is the most extreme case that the material having the largest buildup factor of $\sim 10^{11}$ at 40 mfp is combined with iron of the smallest buildup factor as low as about 4 at the same depth. In this case, the buildup factors in iron in double-layered shields of lead followed by iron decrease moderately to those of the iron monolayer. These buildup factors are

quite well reproduced by the present model.

However, the buildup factors in lead in the double-layered shields of the reversed material order are overestimated by the present model by a factor of 2~4. The gamma-ray spectrum in iron has the largest value at the source energy, and decreases quickly with decreasing the gamma-ray energy. On the other hand, although very big peaks exist in the lead spectrum due to the K-X rays of ~89 keV, the spectrum value above this energy is very small. Therefore, regarding the EGS4 results the gamma-ray buildup in the lead starts with some delays behind the material boundaries after gamma-rays near to the source energy are scattered down to an energy range below the K-edge. In the present model, the region above 80 keV up to 99 keV is in the same energy group, and the above-mentioned detailed spectrum difference between iron and lead is not described. The increase in the buildup factor starts in lead just after the material boundary, which leads to an overestimation of the buildup factor. The increase in the energy group number at a higher energy range is needed to improve the reproducibility of the buildup factors.

The buildup factors are shown in Fig.11 for the combination of water and lead, which is an example of the extreme behaviors of the buildup factor at 0.1 MeV. In this case, the overall agreement of the data between the present model and the EGS4 calculation is better than that for the combination of iron and lead. This is because the energy spectrum of gamma-rays in both lead and water spreads in wider energy groups than in the iron shields, and the spectrum variation between the two materials is better described by the present model.

Interesting behaviors of the buildup factor are pointed out for the double-layered shields. The buildup factor in the 2nd layer of water followed by lead once decreases just behind the material boundary, then starts increasing quickly with the lead thickness. The temporary decrease in the buildup factor is caused by the cutoff of the very low-energy part of gamma-rays that had built up in water. A reversed behavior is seen in the buildup factor of the shields of lead, followed by water, where a temporary excess of the buildup factor to the corresponding data of the lead monolayered shield occurs. The latter behavior is caused by the disappearance of strong absorption at very low energies when the material is changed from lead to water. It should be noted that these interesting behaviors of the buildup factor are very well reproduced by the present model.

IV CONCLUSION

Our modified approximating model of the multilayer gamma-ray buildup factor was tested based on the reference buildup factor data estimated by using EGS4 for very thick shields of up to 40 mfp.

As a conclusion of the tests, it is pointed out that the present approximating model generally has a very good capability to reproduce the multilayer buildup factors, even in very thick shields. The observed error was within 15% in the intermediate energy range, about 30% in the higher energy range, and 35% at 0.3 MeV.

At a very low energy of 0.1 MeV, the error of the approximation reaches a factor of 4 in some cases. However, this error is acceptable as an approximating formula of the buildup factor, considering a very large change of $\sim 10^{11}$ in the buildup factor.

In the next step, the possibility of interpolating the parameters and the matrices with the gamma-ray energy and the Z-number of materials should be tested. Then, a systematic parameterization of the buildup factors will be started for major shielding materials. In parallel with these studies, we will incorporate the current expression into a point kernel

code.

References

- [1] Su, M. F. and Jiang, S. H.:Gamma-ray Buildup Factors for a Point Isotropic Source in Stratified Spherical Shields, *Nucl. Sci. Eng.*, **102**, 64 (1989).
- [2] Harima, Y. and Hirayama, H.:Detailed Behavior of Exposure Dose Buildup Factor in Stratified Shields for Plane-Normal and Point Isotropic Sources, Including the Effects of Bremsstrahlung and Fluorescent Radiation, *Nucl. Sci. Eng.*, **113**, 367 (1993).
- [3] Kitazume, M.:Some Considerations of Buildup Factors in Gamma-ray Penetration for Multilayers, *Nippon Genshiryoku Gakkaishi*, **7**, 496 (1965). (in Japanese)
- [4] Harima, Y. and Nishiwaki, Y.:An Approximate Transmission Dose Buildup Factor for Stratified Slabs, *J. Nucl. Sci. Technol.*, **6**, 711 (1969).
- [5] Bowman, L. A. and Trubey, D. K.:Monte Carlo Calculation of Gamma-ray Dose-Rate Buildup Factors for Lead and Water Shields and Monte Carlo Calculation of the Deposition of Gamma-ray Heating in Stratified Lead and Water Slabs, *ORNL-2609*, Oak Ridge National Laboratory (1958).
- [6] Kalos, M. H. quoted in Goldstein, H.:*Fundamental Aspect of Reactor Shielding*, p.225, Addison-Wesley Publishing Co. Inc., Reading, Massachusetts (1959).
- [7] Broder, D. L., Kayurin, Yu. P. and Kutrezov, A. A.:Transmission of Gamma Radiation through Heterogeneous Media, *Sov. At. Energy*, **12**, 26 (1962).(English Translation)
- [8] Penkuhn, H.:A Parametric Representation of Gamma-ray Attenuation in Two-Layer Shields, *Nucl. Sci. Technol.*, **1**, 809 (1979).
- [9] Harima, Y., Hirayama, H., Tanaka, S. and Sugiyama, M.:The Behavior of Gamma-ray Buildup Factors in Stratified Shields, *Proc. Topl. Mtg. New Horizons in Radiation Shielding*, Pasco, Washington, April 26-May 1, 1992, p.473 (1992).
- [10] Shin, K. and Hirayama, H.:A New Approximating Model for Gamma-ray Buildup Factors of Stratified Shields, *Nucl. Sci. Eng.*, **118**, 91 (1994).
- [11] Shin, K. and Hirayama, H.:Approximating Model for Multilayer Gamma-ray Buildup Factors by Transmission Matrix Method: Application to Point Isotropic Source geometry, *Nucl. Sci. Eng.* **120**, 211 (1995).
- [12] Nelson, W. R., Hirayama, H. and Rogers, D. W. O.:The EGS Code System, *SLAC-265*, Stanford Linear Accelerator Center, Stanford (1985).
- [13] Hirayama, H.:calculation of Gamma-ray exposure buildup factors up to 40 mfp using the EGS4 Monte Carlo Code with a Particle Splitting, *J. Nucl. Sci. Technol.*, **32**, 1201 (1995).
- [14] Hirayama, H. and Shin, K.:Application of the EGS4 Monte Carlo Code to a Study of Multilayer Gamma-ray Exposure Buildup Factors up to 40 mfp, submitted to *J. Nucl. Sci. Technol.*

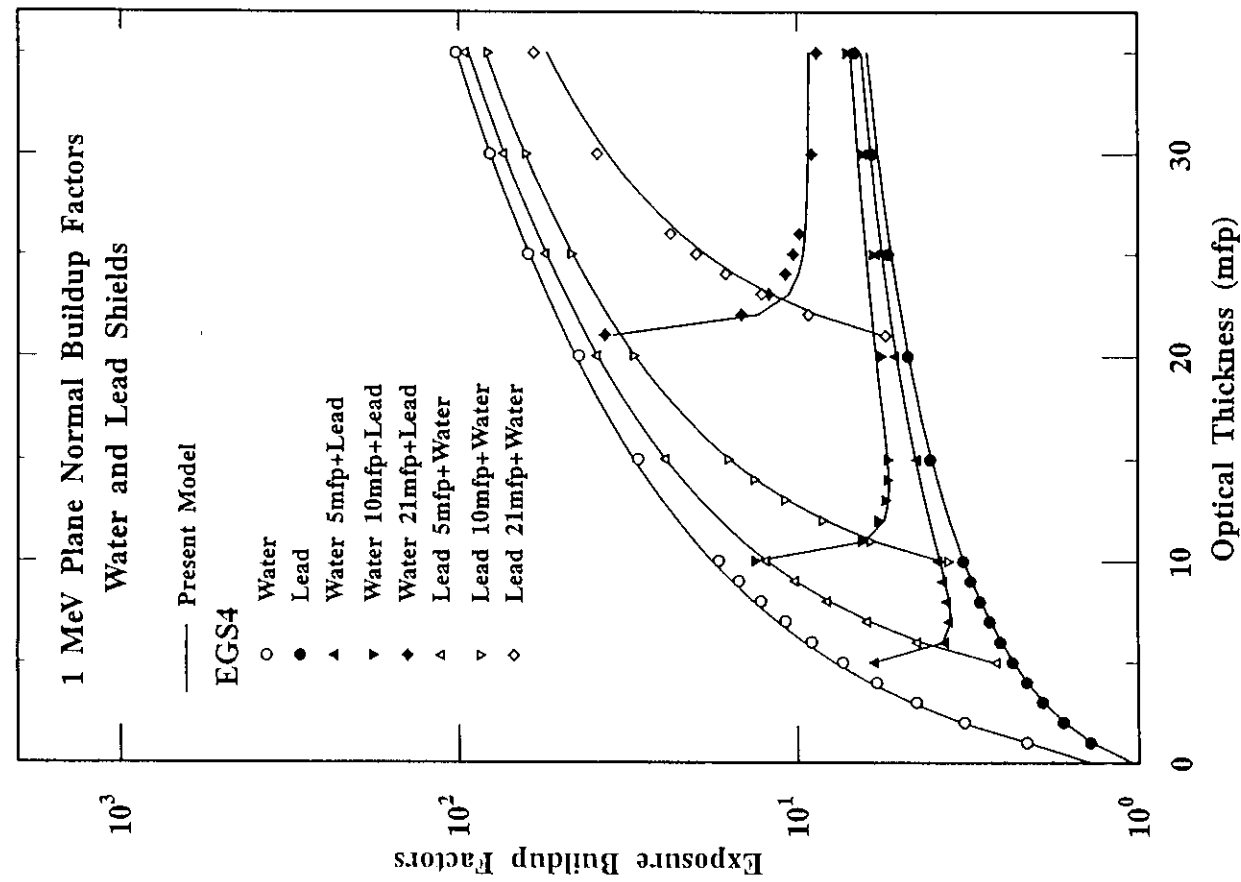


Figure 1 Plane normal buildup factors at 1 MeV for single- and double-layered shields of water and lead.

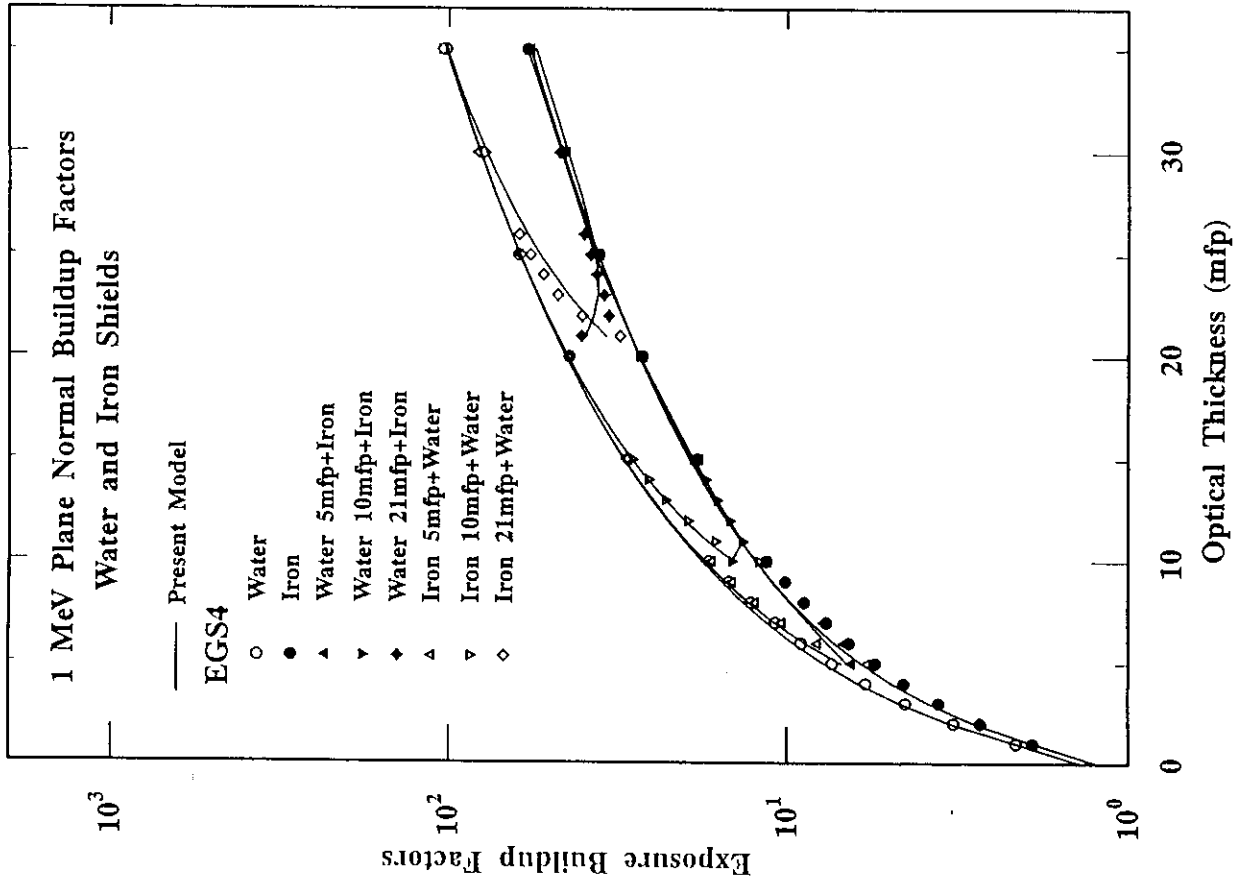


Figure 2 Plane normal buildup factors at 1 MeV for single- and double-layered shields of water and iron.

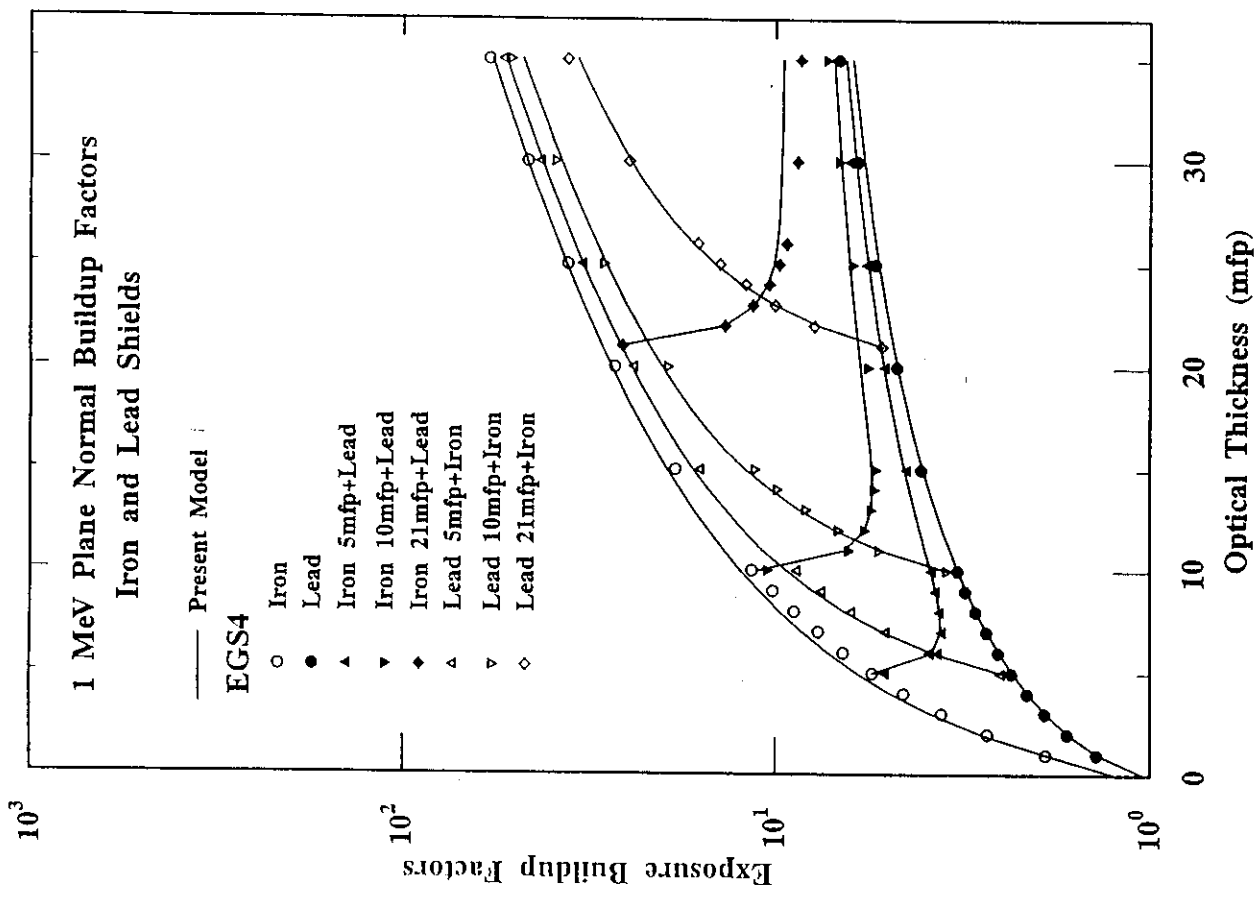


Figure 3 Plane normal buildup factors at 1 MeV for single- and double-layered shields of iron and lead.

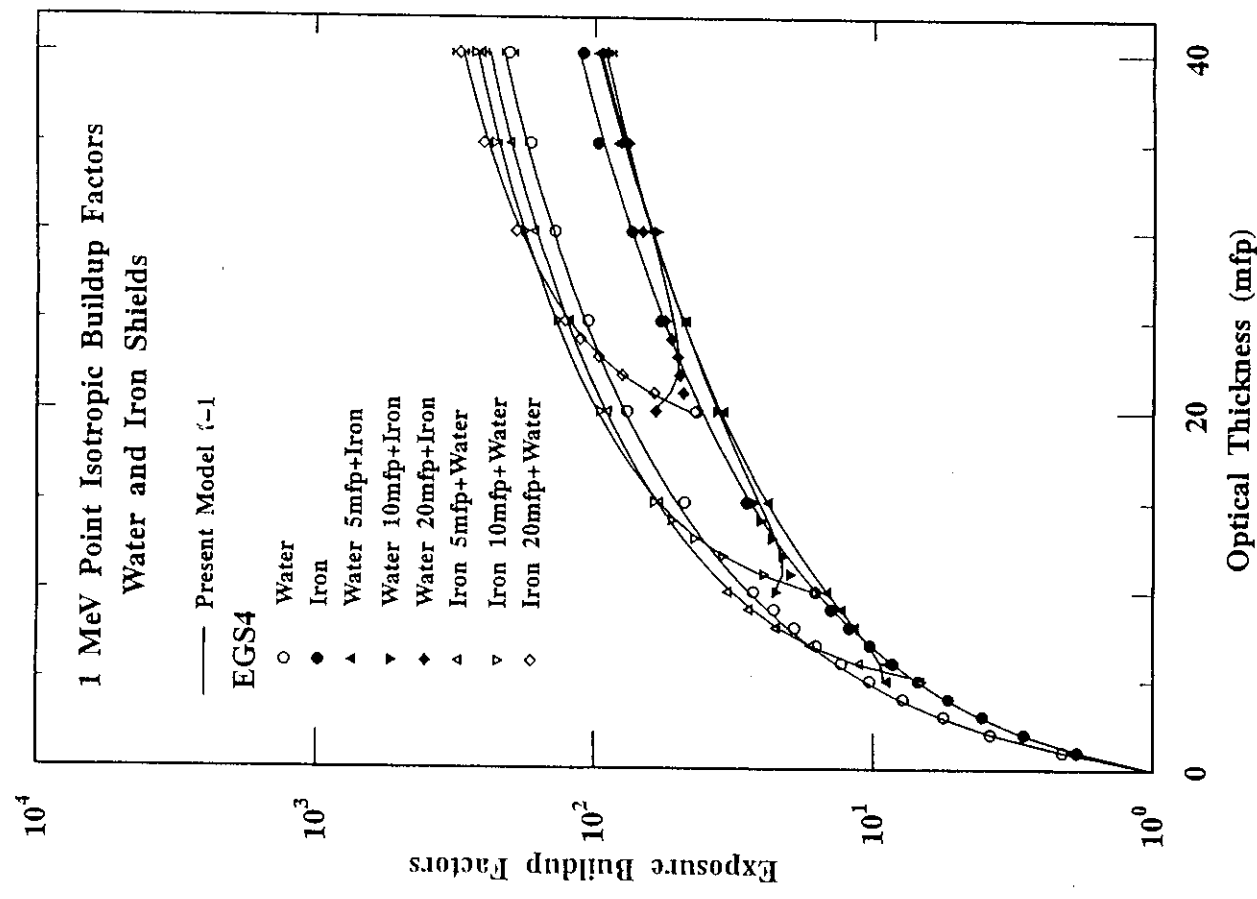


Figure 4 Point isotropic buildup factors at 1 MeV for single- and double-layered shields of water and iron.

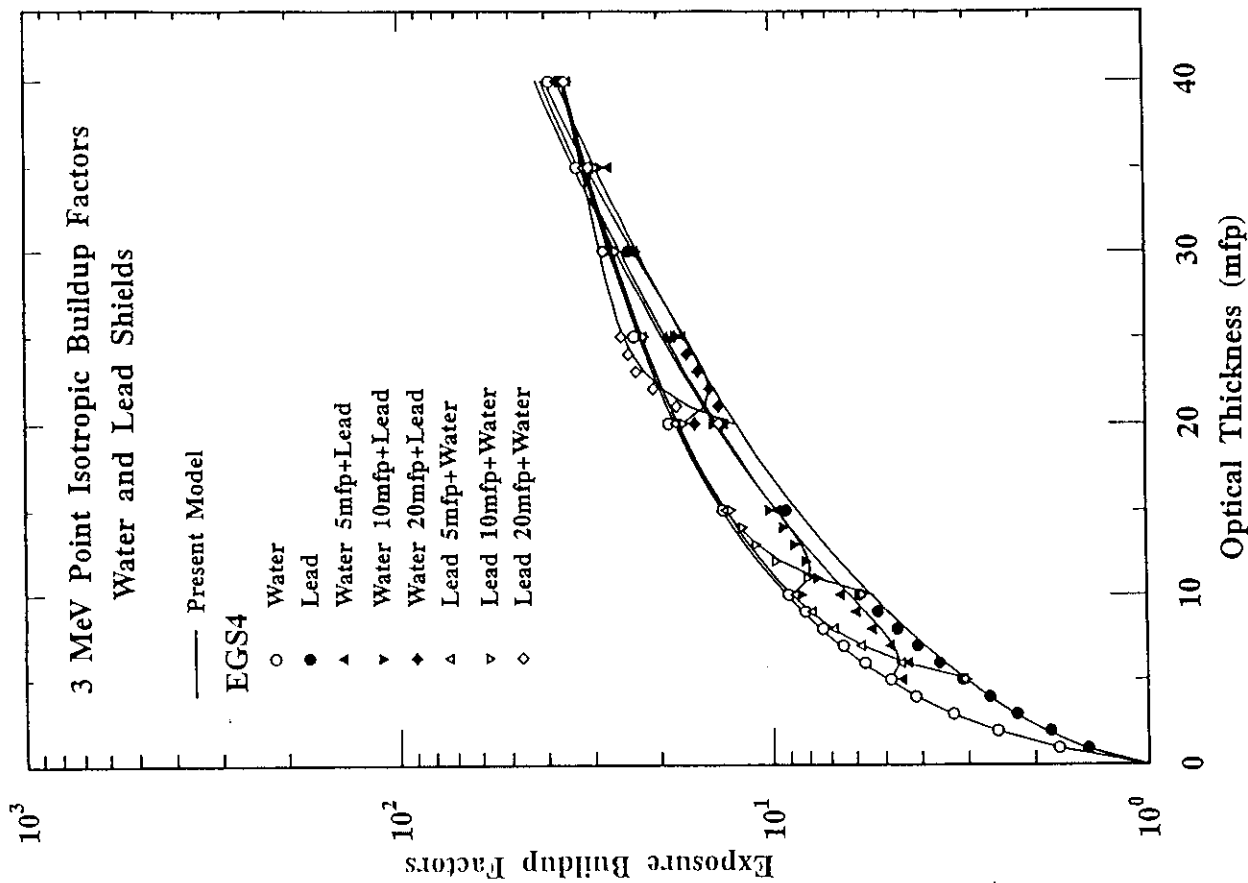


Figure 5 Point isotropic buildup factors at 3 MeV for single- and double-layered shields of water and lead.

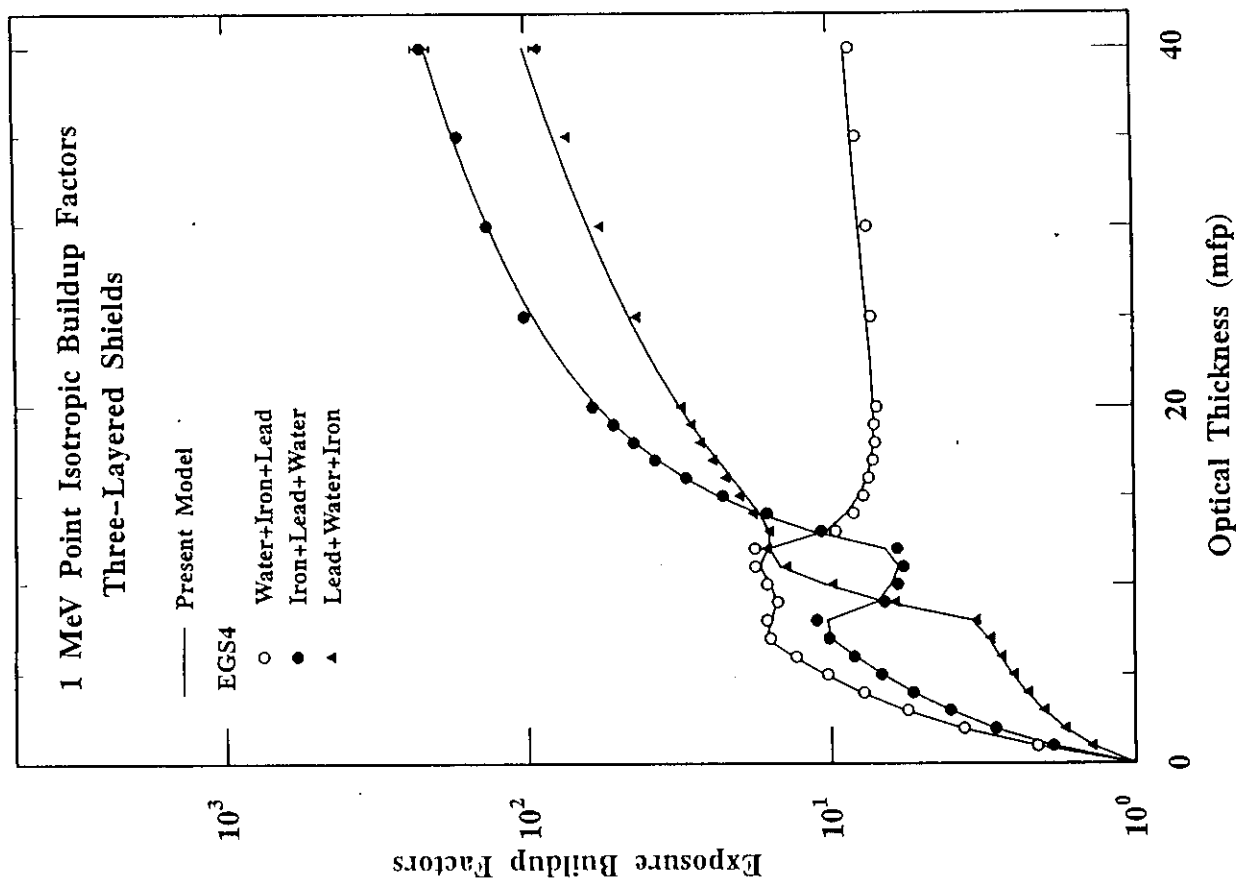


Figure 6 Point isotropic buildup factors at 1 MeV for 40-mfp thick triple-layered shields, water+iron+lead, iron+lead+water and lead+water+iron, whose 1st layer thickness is 8 mfp and 2nd layer thickness is 4 mfp.

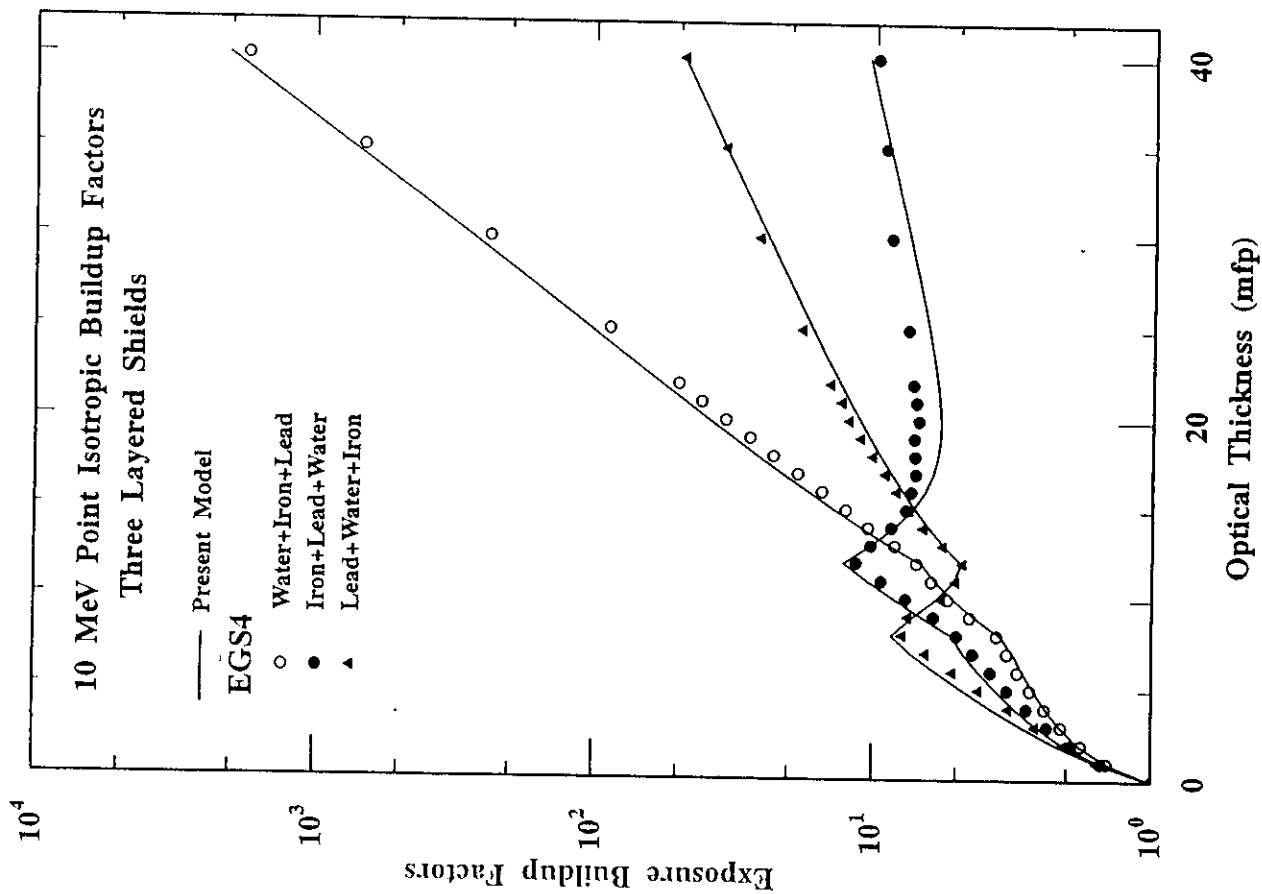


Figure 8 Point isotropic buildup factors at 10 MeV for 40-mfp thick triple-layered shields, water+iron+lead, iron+lead+water and lead+water+iron, whose 1st layer thickness is 8 mfp and 2nd layer thickness is 4 mfp.

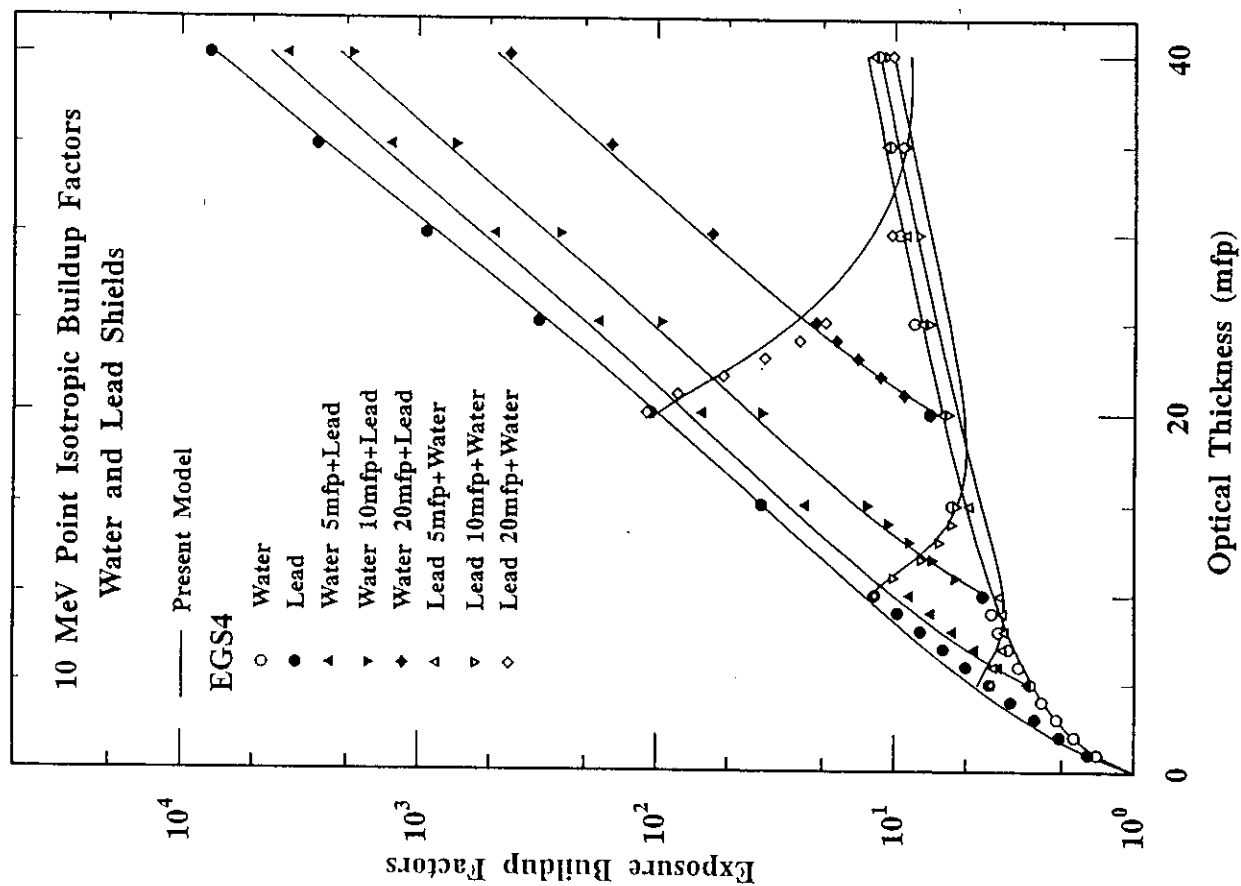


Figure 7 Point isotropic buildup factors at 10 MeV for single- and double-layered shields of water and lead.

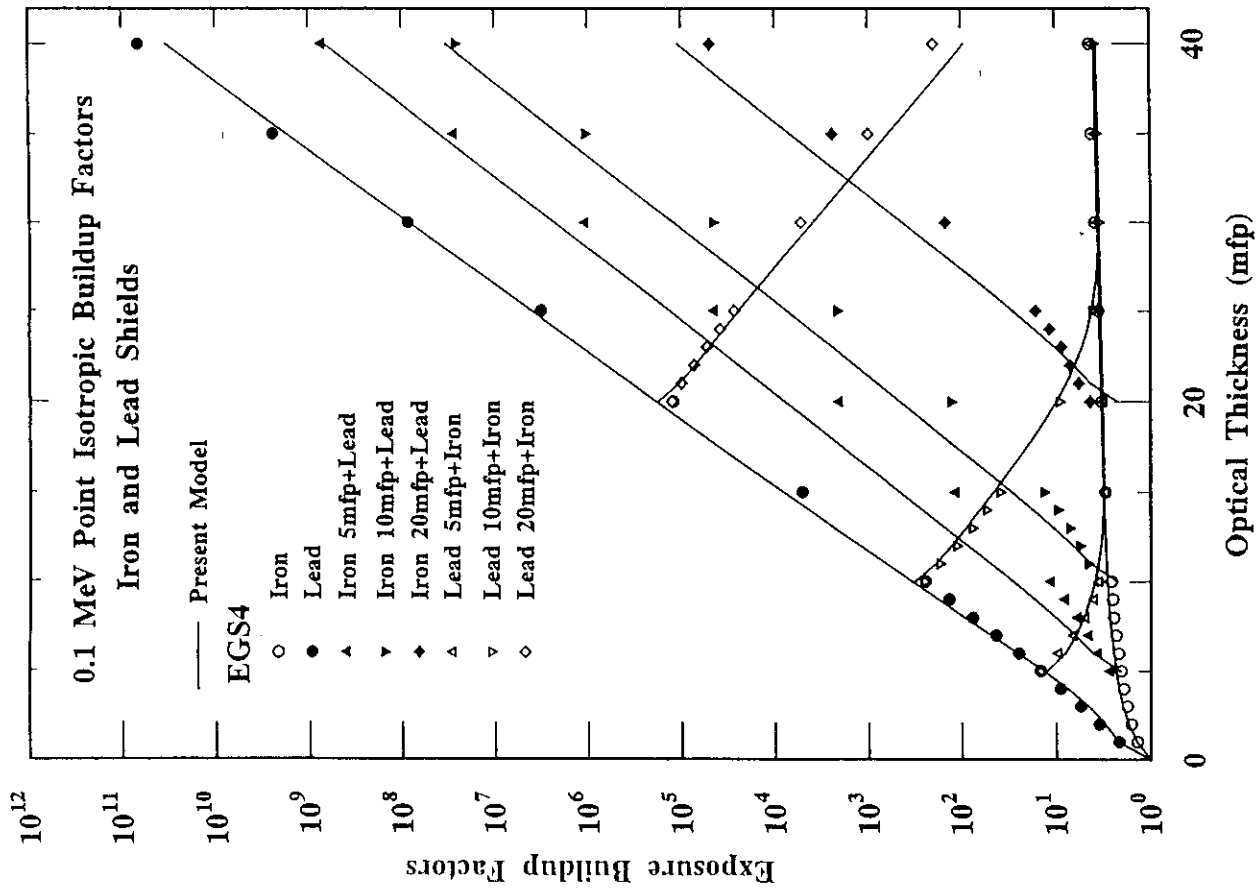


Figure 10 Point isotropic buildup factors at 0.1 MeV for single- and double-layered shields of iron and lead.

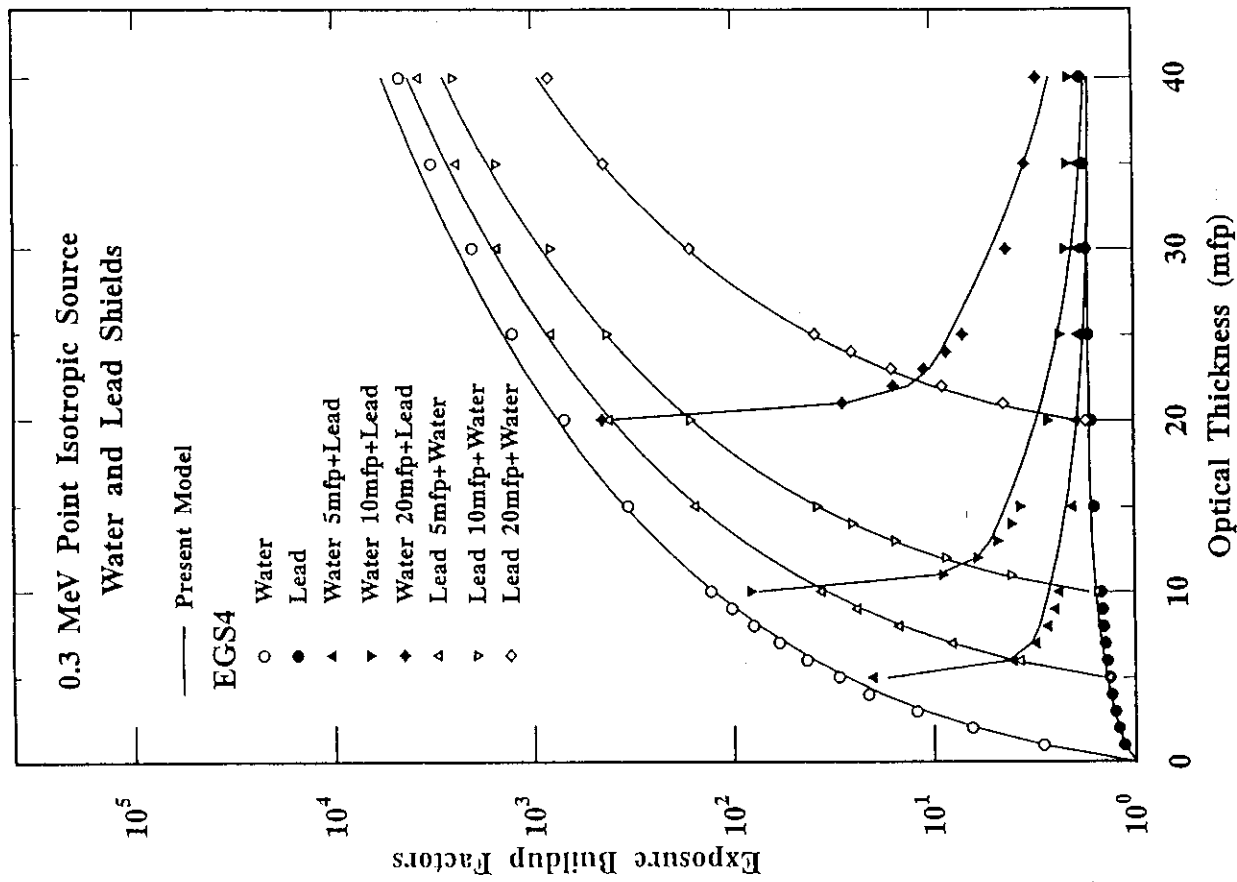


Figure 9 Point isotropic buildup factors at 0.3 MeV for single- and double-layered shields of water and lead.

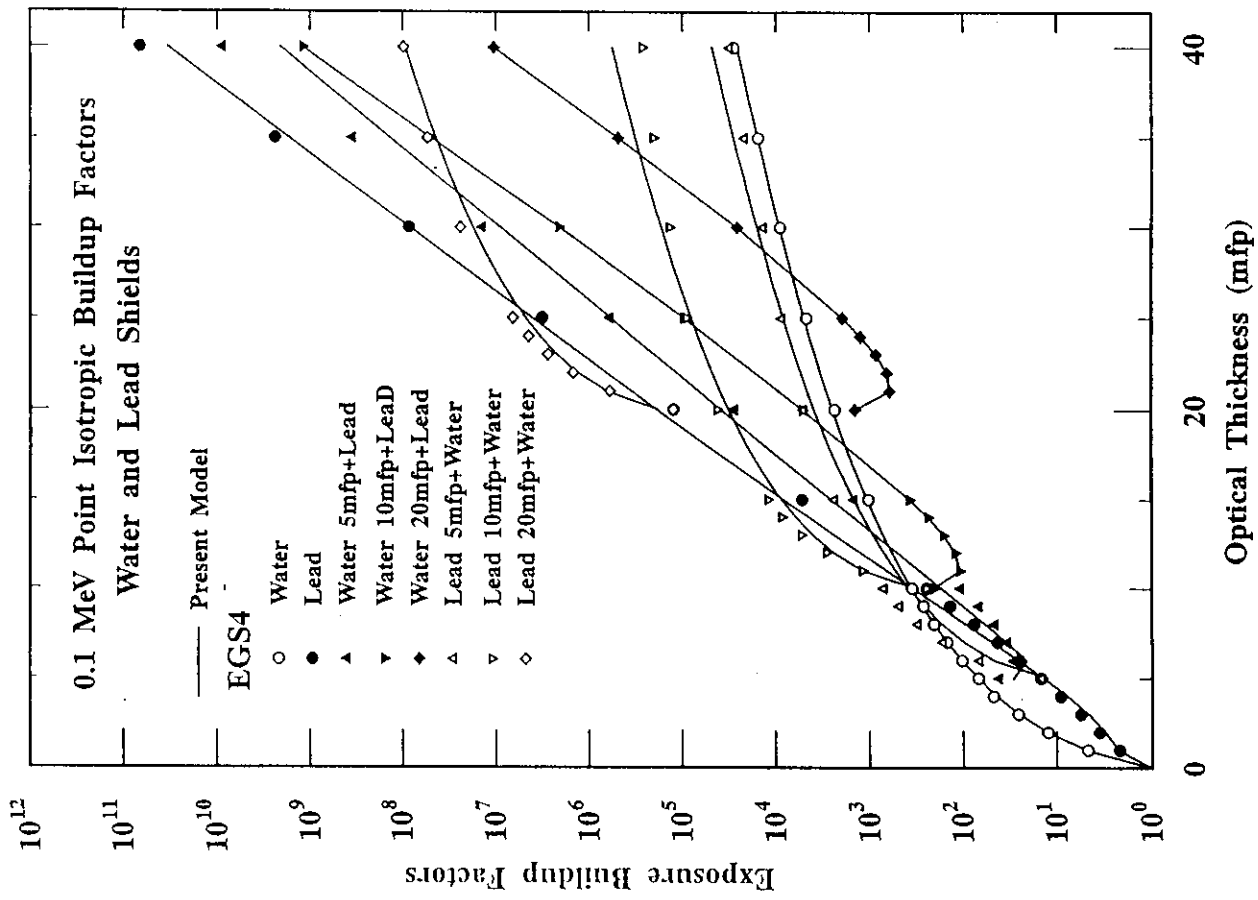


Figure 11 Point isotropic buildup factors at 0.1 MeV for single- and double-layered shields of water and lead.